



Numerical simulation of the effect of particle size on the erosion damage in ball valves of pressure reducing station

Amir Askari ^{1,*}, Ali Falavand Jozaei ¹

¹Department of Mechanical Engineering, Ahvaz Branch, Islamic Azad University, Ahvaz, Iran

Abstract

Ball valve has many applications in industry especially in gas delivery system such kind of valve is categorized as on - off flow control valve. Present study aims to investigate unusual application of ball valve to control fluid flow in industry and its destructive effect including erosion of ball and body of the valve. Simulation of ball valve is done using ANSYS Fluent software in which effect of erosion is investigated in different working conditions. In this article, working condition for two different concentrations of suspended particles as well as four ball positions in different angles are considered in addition the effects of increased particle diameter on the rate of erosion for three diameters (3.86 μm , 267.45 μm and 531.03 μm) in four conditions of valve (25%, 50%, 75% and 100%) and two different concentrations of particle (3% and 6%) are assessed. It is shown that rate of erosion is increased with increase of particle diameters in 25%, 50% and 75% open state of valve. On the contrary, the results showed that opposite rule governs complete open state. Furthermore, it is demonstrated that increase in particle diameter decreases the area of erosion in four conditions of valve.

Keywords: Ball valve, Erosion, Particle diameter, Simulation

1. Introduction

In ball valve the flow blocker is a spherical or half- spherical member which rotates 90 degree by stem around a vertical axis with regard to the direction of fluid. On the sphere, a hole is embedded. If the hole is open, it is in the direction of the flow channel and when closed, it is perpendicular to the path. When the ball is in the state other than above mentioned state, turbulent flow is made in the valve. This limits the application of ball valve and causes problems such as erosion.

Researches carried out at out erosion are as follows:

Haugen et al. [1] studied erosion on choke valves and showed that erosion can be reduced by selecting durable materials and optimizing the design. They selected and investigated 28 different materials. McLaury et al. [2] employed the API RP 14E method to study erosion and the methods used for its limitation. Forder et al. [3] investigated erosion in control valves and showed that in addition to erosion, presence of suspended solid particles in the fluid causes the valve to lose its controlling capabilities. Parslow et al. [4] studied erosion in a tee caused by presence of solid particles and reported that factors such as the number of particles, velocity, and particles collision angle can control erosion. In their study, Kavner et al. [5] investigated the phase stability and density of FeS at different pressures and temperatures. Jin et al. [6] carried out erosion numerical simulation in tube due to particle collision in which useful results such as redundancy distribution of particle collision and erosion of tube were obtained. Oka et al. [9] showed that intensity of erosion is affected by the compactness and

* Corresponding Author. Tel.: +98 9106333840
Email Address: AmirAskari36@yahoo.com

pulses of suspended particles and proved that the velocity and collision angle of particles significantly affect corrosion erosion. Habib et al. [11] investigated erosion in heat exchangers and assessed the effect of flow velocity and particle sizes on erosion. They proved that erosion rate is related to the particles velocity and particle size in erosion is significant. Malka et al. [12] showed that erosion leads to corrosion and wear, while corrosion and erosion increase wear. Shahbazi and Noori zadeh [19] conducted studies on the black powder present in natural gas transmission network and introduced the ingredients of this powder using different techniques and methods. Shafee et al. [20] used CFD to numerically analyze erosion in pipelines and gas stations. Zhu et al. [21] assessed erosion in needle valves and investigated the effect of factors such as fluid inlet velocity, concentration, diameter and shape of particles on erosion. They believed that valve lifetime can be extended by altering the shape of particles or their velocity at the inlet. Moreover, they suggested that changing the diameter of particles has the most significant effect on erosion reduction. Droubi et al. [22] studied erosion caused by collision of suspended particles in elbow and showed that factors such as equipment shape, flow conditions, and suspended particles play a significant role in erosion. Flow erosion is a highly complicated issue due to a number of parameters including operation, structure and fluid parameters affecting the erosion severity, such as flow velocity, flow channel structure, fluid properties, particle diameter and particle concentration [10], [14]. Fan et al. [7], Suzuki et al. [13], Tang et al [14], Li et al. [16] and Yan et al. [17] investigates has been carried out in attempts to explain flow erosion by physical or numerical modeling. Zhang et al. [18] conducted numerical investigation of the location of maximum erosive wear damage in elbow. Deng et al. [8] carried out experiments with four bend orientations to investigate the effect of bend orientation on puncture point location. Ferng and Lin [15] pointed out that the geometry of flow channel presents obvious effect on flow erosion. However, the majority of these investigations focus on the erosion of pipe bends elbows and tees whereas limited number of them has been conducted on valves. Specifically, no studies were conducted on erosion in ball valves.

2. Explanation of Problem

Let 's consider a ball valve with internal diameter of 400 mm and length of assembly till two flange heads equal to 762 mm. In order to prevent reverse flow, domain is elongated about 1 meter from both sides. Valve is simulated with rotation of ball in four open conditions including complete open, half- open, 75% open and 25% open states, and two particle concentrations are considered in each state. Base fluid along with solid particles enter a valve from one side, and after through the path, hitting the ball, and making erosion, leaves the valve from other side. Base fluid is defined as compressible according to laws of ideal gas. Suspended FeS particles are inert and spherical. Using uniform model for each state the distribution of particles with three different diameters (3.86 μm , 267.45 μm and 531.03 μm) [19] are chosen and then rate of erosion is calculated.

Table 1 show the Physical and mechanical properties for suspended particles and valve.

Table1. Physical and mechanical properties for particle and valve

Density of Fes (kg/m^3)	Roughness of Valve (mm)	Diameter of particle (μm)		
		min	mean	max
5960 [5]	0.05	3.87	267.45	531.03

Table 2 show the operation condition, mass flow rate of particles (in three states) used in simulation.

Table2. Simulation cases

Case	operation condition		\dot{m} particle(kg/s)	P _{in} (bar)	P _{out} (bar)
	V(m/s)	valve opening(%)			
1	13	100	0.0395-3%	28.19	27.94
2	13	100	0.0798-6%	28.19	27.94
3	16	75	0.0362 – 3%	28.19	27.9
4	16	75	0.0724 – 6%	28.19	27.9
5	23	50	0.0348 – 3%	28.19	27.7
6	23	50	0.0696 – 6%	28.19	27.7
7	45	25	0.0333 – 3%	28.19	25.9
8	45	25	0.0665 – 6%	28.19	25.9

3. Governing Equations and Numerical Method

3.1. Governing Equations

Three main steps are involved in CFD-based erosion:

Flow modeling, particle tracking, erosion computation. First, gas is seamed as continuous fluid phase evaluated by a Navier–Stokes solver, and solid particles are treated as spherical particles with uniform diameter added into continuous phase flow field as discrete phase, which are captured by discrete phase model (DPM). And particle are inert are assumed in simulation.

The mass and momentum conservation equations used in the continuous fluid flow model are given in Eqs. (1) and (2), respectively [21]:

$$\nabla \times (\rho_f \mathbf{v}) = 0 \quad (1)$$

$$\nabla \times (\rho_f \mathbf{v} \mathbf{v} - \boldsymbol{\tau}_f) = \mathbf{f}_f \quad (2)$$

In which,

$$\boldsymbol{\tau}_f = \left[-p + \left(-g - \frac{2}{3}\mu \right) \nabla \times \mathbf{v} \right] \mathbf{I} + 2\mu \mathbf{E} \quad (3)$$

$$\mathbf{E} = \frac{1}{2} (\nabla \mathbf{v} + \nabla \mathbf{v}^T) \quad (4)$$

Where \mathbf{V} is velocity of gas, ρ_f is density of gas, \mathbf{f}_f is volume force of fluid, $\boldsymbol{\tau}_f$ is stress of fluid, P is pressure, μ is dynamic viscosity, \mathbf{I} is second order unit tensor and g is gravitational acceleration.

And for equations of k- ϵ turbulence model [21]:

$$\frac{\partial (\rho_f k v_i)}{\partial x_i} = \frac{\partial}{\partial x_j} \left[\left(\mu + \frac{\mu_t}{\sigma_k} \right) \frac{\partial k}{\partial x_j} \right] + G_k + G_b - \rho_f \epsilon - Y_M \quad (5)$$

$$\frac{\partial (\rho_f \epsilon v_i)}{\partial x_i} = \frac{\partial}{\partial x_j} \left[\left(\mu + \frac{\mu_t}{\sigma_\epsilon} \right) \frac{\partial \epsilon}{\partial x_j} \right] + \rho_f C_1 S \epsilon - \rho_f C_2 \frac{\epsilon^2}{K + \sqrt{v \epsilon}} + c_{1\epsilon} \frac{\epsilon}{K} C_{3\epsilon} G_b \quad (6)$$

In which,

$$C_1 = \max \left(0.43, \frac{\eta}{\eta + 5} \right) \quad (7)$$

$$\eta = (2S_{ij} \times S_{ij})^{\frac{1}{2}} \frac{K}{\epsilon} \quad (8)$$

$$S_{ij} = \frac{1}{2} \left(\frac{\partial v_i}{\partial x_j} + \frac{\partial v_j}{\partial x_i} \right) \quad (9)$$

where the subscripts i and j indices for coordinate axes, k and ε refer to turbulent kinetic energy and turbulent kinetic energy dissipation rate per unit mass, respectively, σ_k and σ_ε present Prandtl number corresponding to turbulent kinetic energy and Prandtl number corresponding to turbulent kinetic energy dissipation rate, respectively. Y_M is impact of compressible turbulence inflation on the total dissipation rate, ν is molecule kinetic viscosity, G_k is production term of turbulent kinetic energy due to the average velocity gradient, G_b is production term of turbulent kinetic energy due to lift and $C_{1\varepsilon}$, C_2 and $C_{3\varepsilon}$ are empirical constants taken as 1.44, 1.9 and 0.09, respectively [21].

After continuous phase flow field such as velocity and pressure distribution obtained by solving the above equations, the particle dynamics are treated in a Lagrangian framework according to the particle equation of motion, including the trajectory of particles, the attack angle and velocity perturbation [21].

This particle motion equation is called as DPM model and is specified as

$$\frac{dv_s}{dt} = \frac{C_D Re_{d_s}}{24\tau_t} (v - v_s) + \frac{g(\rho_s - \rho_f)}{\rho_s} + 0.5 \frac{\rho_f}{\rho_s} \frac{d(v - v_s)}{dt} \quad (10)$$

In which,

$$\tau_t = \frac{\rho_s d_s^2}{18\mu} \quad (11)$$

$$Re_{d_s} = \frac{\rho_f d_s |v_s - v|}{\mu} \quad (12)$$

$$C_D = \frac{24}{Re_{d_s}} (1 + b_1 Re_{d_s}^{b_2}) + \frac{b_3 Re_{d_s}}{b_4 + Re_{d_s}} \quad (13)$$

Where ρ_s is density of particle, d_s is diameter of particle, v_s is velocity of particle, Re_{d_s} is particle equivalent Reynolds number, C_D is drag coefficient, τ_t is particle relaxation time, b_1 , b_2 , b_3 and b_4 are constants taken as 0.186, 0.653, 0.437 and 7178.741, respectively.

We can simply write the DPM relation without considering the effect of gravity:

$$\frac{du_p}{dt} = F_D (\vec{u} - \vec{u}_p) \quad (14)$$

In which,

$$F_D = \frac{18\mu_m C_D Re}{\rho_p d_p^2} \quad (15)$$

The force that was exerted on the secondary phase is drag force that was exerted by fluid, and value of C_D coefficient is a function of Reynolds number. If the particle shape is considered spherical [22], we have:

$$C_D = a_1 + \frac{a_2}{Re} + \frac{a_3}{Re^2} \quad (16)$$

In order to calculate the rate of erosion, we can use mathematical model that makes the effect of above- mentioned different parameters dependent on the rate of erosion. The mathematical model and its inner parameters are as follows

$$ER = \sum_{p=1}^{N_{particles}} \frac{C_d V^n f(\alpha) \dot{m}}{A_{face}} \quad (17)$$

Where ER is mass of material loss per unit area per unit time, C_d is Particle diameter function, V is Particle impact velocity, n is Velocity exponent, $f(\alpha)$ is impact angle function and \dot{m} is Particle mass flow rate.

3.2. Numerical Method

Simulation of above equations could be done by using ANSYS Fluent 15 software which covers all models and related equations. Numerical method used in this software is finite

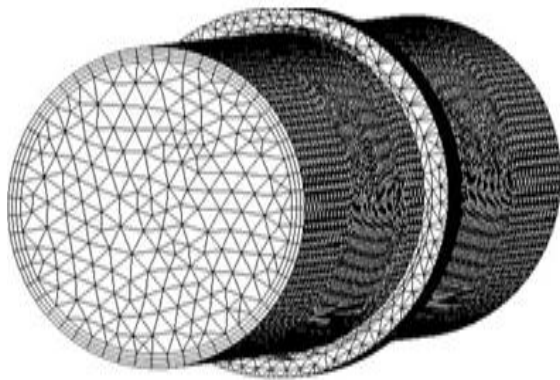
volume according to which we should produce the computational mesh in the proper range and solve the above equations with proper boundary conditions. This software allows the designer to define all parameters of fluid material as well as properties of particles.

The type of solver used in this problem is steady state with simple algorithm without considering the gravity effect. Furthermore, second- order upwind with acceptable accuracy is used for spatial discretization.

3.3. Computational Mesh

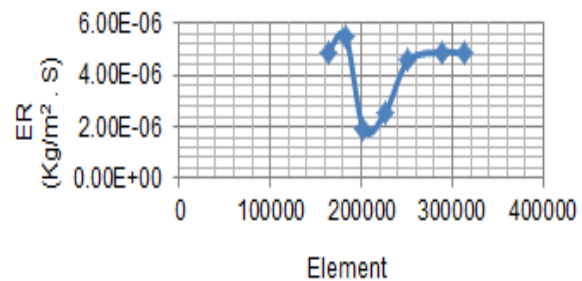
The generated mesh is chosen as a hybrid type the cells near to wall are prism type and has inflation layers and growth factor to calculate boundary layer while the cells far from wall are tetra type. To establish such mesh three layers and growth factor of 1.1 are used (figure 1 a).

Analysis is done in seven steps due to independence of mesh. When the number of mesh is increased at each step, the rate of erosion is calculated. In the last step, rate of error is decreased to 0.821 that is shown in the figure 1 b.



a

Figure.1a.diagram of mesh



b

Figure.1b.diagram of Computational mesh

4. Validation

In order to verify the flow modelling capabilities, a verification study is performed on a 90° elbow with the specific parameters used are shown in Table 3. By comparing the predicted erosion rate with the published work of Droubi [22], the accuracy of the flow solution can be assessed. The shape of the contour plots of erosion shown in Figure 2.

The similarities in the erosion profiles illustrate that the results collated in the test cases will provide valid qualitative data to analysis erosion.

Table 3: Validation Test Parameters

Pipe Diameter (m)	Bend Radius (m)	Carrier Fluid Velocity (m/s)	Carrier Fluid	Particle Diameter (m)	Particle Density (kg/m ³)	Sand Production Rate (kg/day)
0.0508	1.5D	15.24	Methane Gas	150 μm	2650	4.55

Rate of erosion is drawn after arrangement and solution.

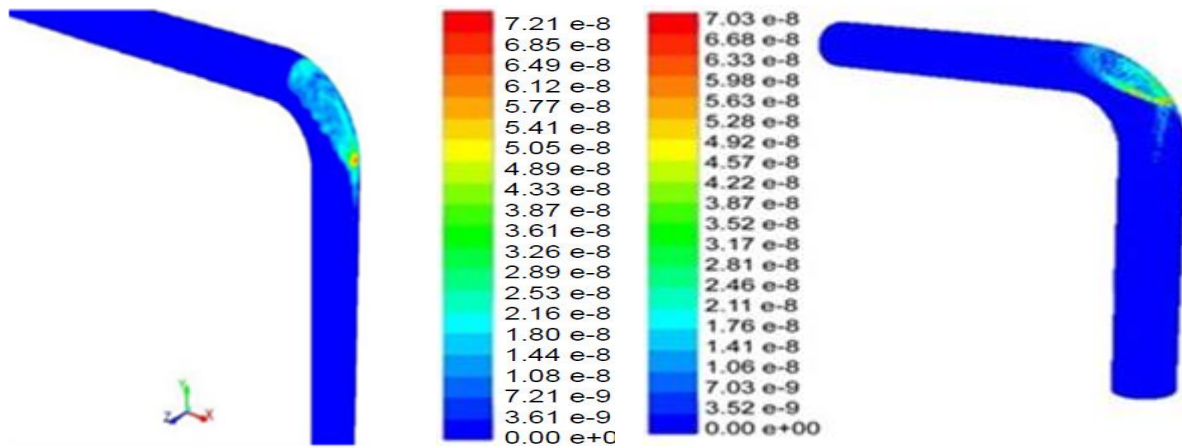


Figure.2.contour of ER for validation

The erosion rate was calculated $7.21e^{-8}$ ($\text{kg}/\text{m}^2.\text{s}$) by Droubi [22] and the amount of erosion rate acquired $7.03e^{-8}$ ($\text{kg}/\text{m}^2.\text{s}$) in this research.

The obtained results are in agreement with analyses done for validation and its rate of error is less than 2.5%.

5. Results and discussion

Effect of Change in Particles Diameter

In this section, four ball conditions in 3% and 6% concentrations were investigated and for each case and particles distribution with three different diameters ($3.86 \mu\text{m}$, $267.45 \mu\text{m}$, $531.03 \mu\text{m}$) [19] was considered and then rate of erosion is calculated.

Due to identical velocities at the outlet for three diameters in all ball conditions, the experiments were not repeated and the output velocities were compared with respect to the ball conditions.

5.1. Particle concentration: 3%

In figures 3 a, b, and c, velocity increases after the ball. Location which occurs due to reduction in cross- section and occurrence of turbulence. Figure d shows complete openness of valve. The speed is constant in all parts due to lack of change in cross- section.

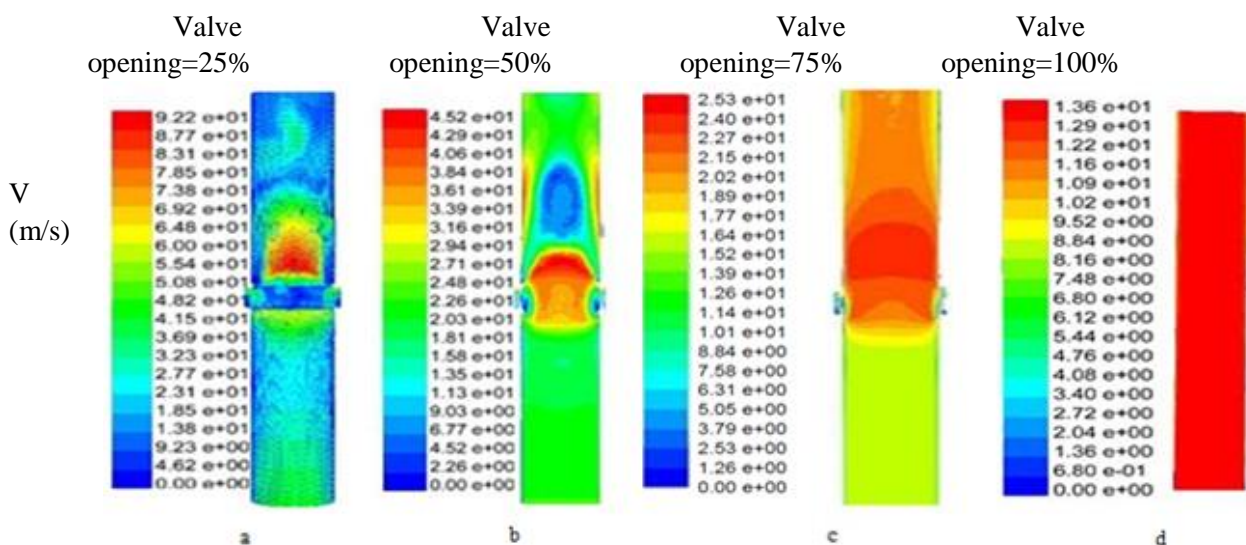


Figure.3.contour of velocity

Contour of erosion rate

5.1.1. Valve opening: 25%, 50% and 75%

In figure 4, due to increase in rate of erosion centralization of area, particle diameters and erosion rate for three states of 25%, 50% and 75% of valve opening are expected.

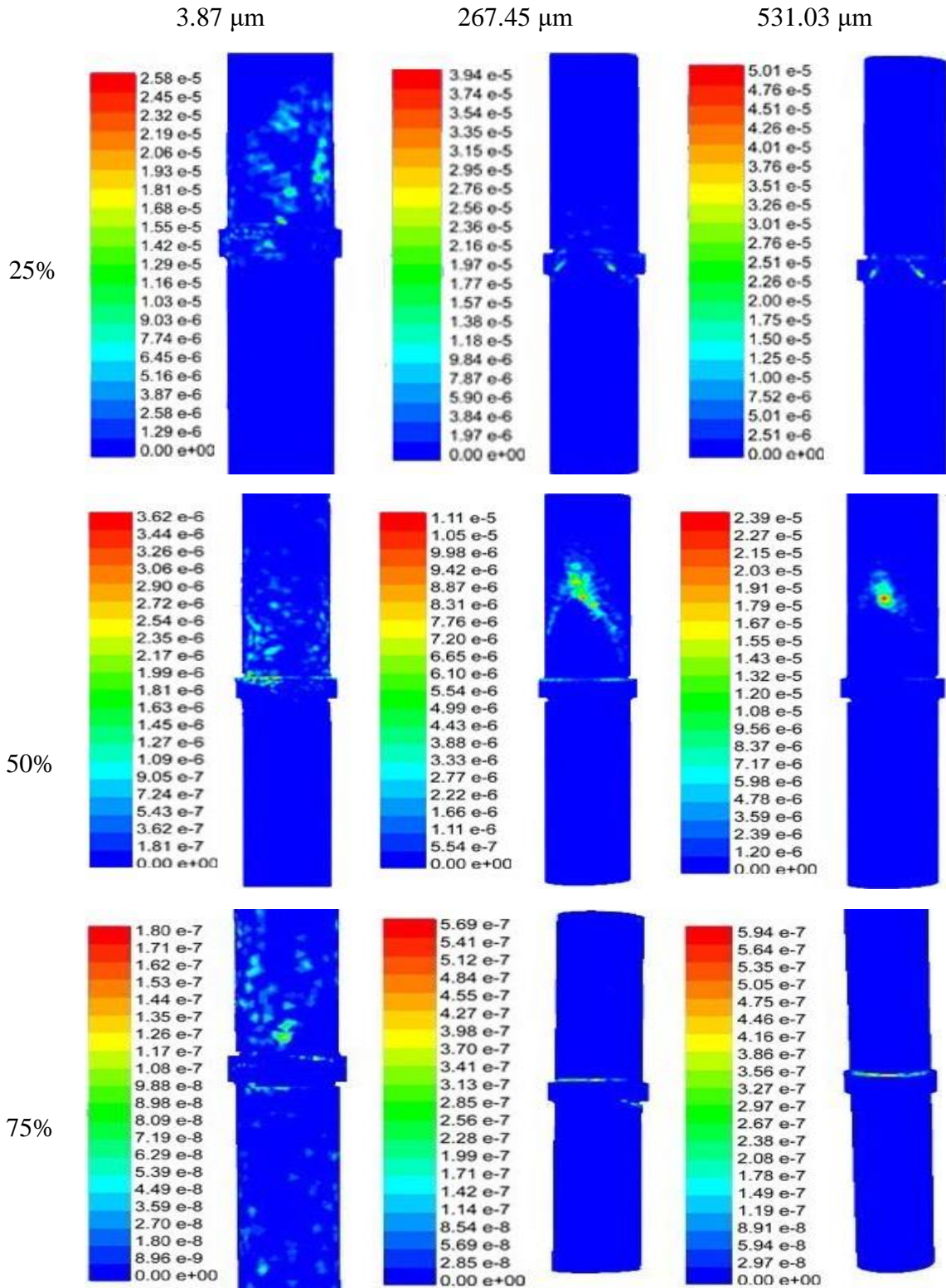


Figure.4. Effects of particle diameter on ER for 3% of particle concentration

5.1.2. Valve opening: 100%

In complete open state (figure 5), the erosion area is more centralized with increase in particle diameter, but the rate of erosion is decreased. This can be due to effect of sliding erosion.

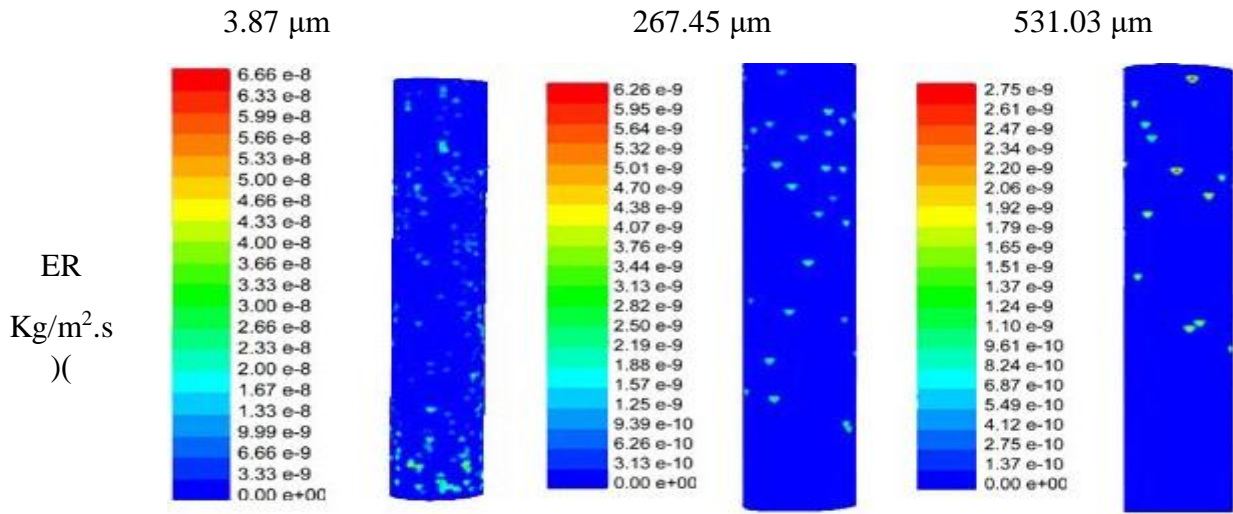


Figure.5. Effects of particle diameter on ER for 3% of particle concentration

For validation of results, the experiment was also repeated for 6% concentration.

5.2. Particle concentration: 6%

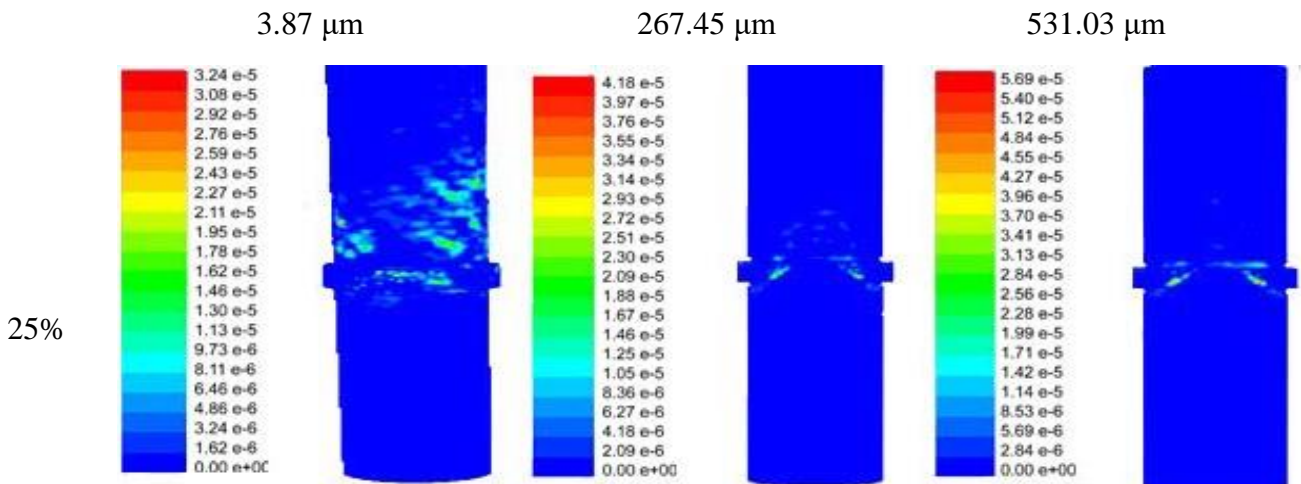
5.2.1. Valve opening: 25% and 50%

Due to increase in particle diameters erosion rate and centralization of area for two states of 25%, 50% of valve opening are increased (figure 6).

Again the range of results is the same as previous step (figure 7). It is observed that for three states of 25%, 50% and 75% of valve opening, the similar results are drawn which indicates the increase in rate of erosion and centralization of area due to increase in particle diameters.

5.2.3. Valve opening: 100%

In 100% open state are observed reduction in rate of erosion and centralization of area with increase in diameter of particles (Figure 8).



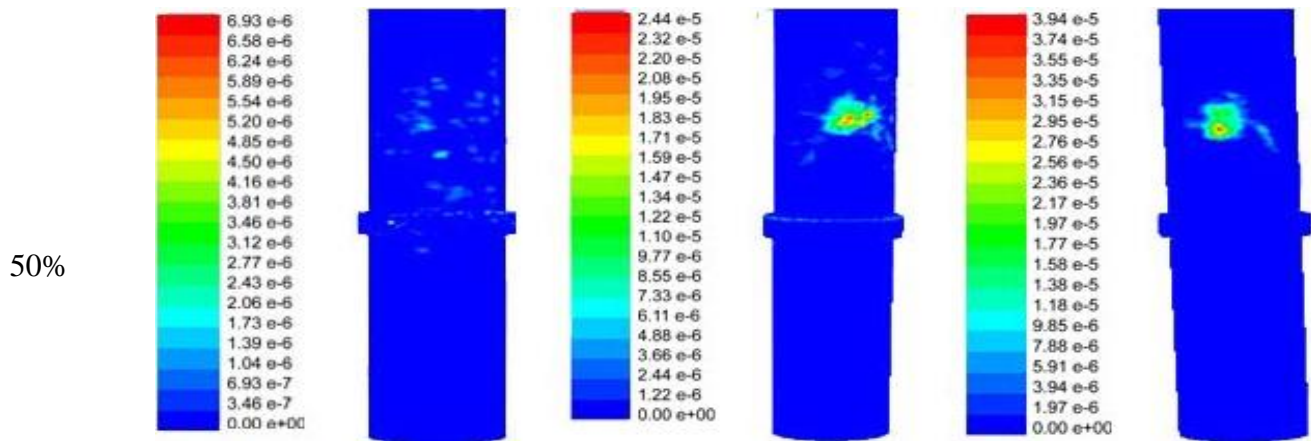


Figure.6. Effects of particle diameter on ER for 6% of particle concentration

5.2.2. Valve opening: 75%

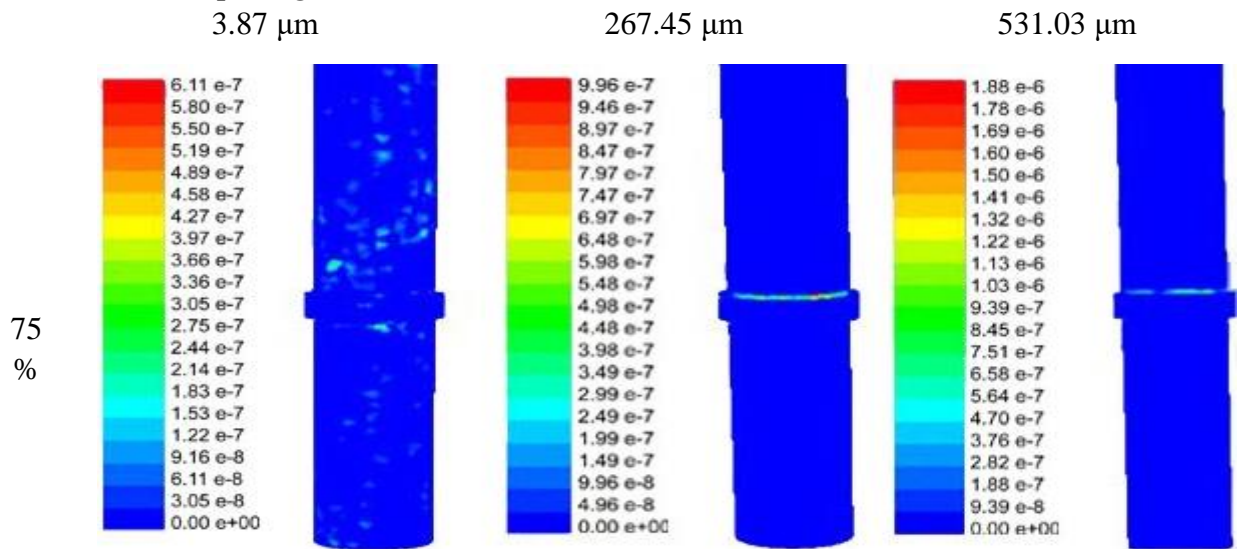


Figure.7. Effects of particle diameter on ER for 6% of particle concentration

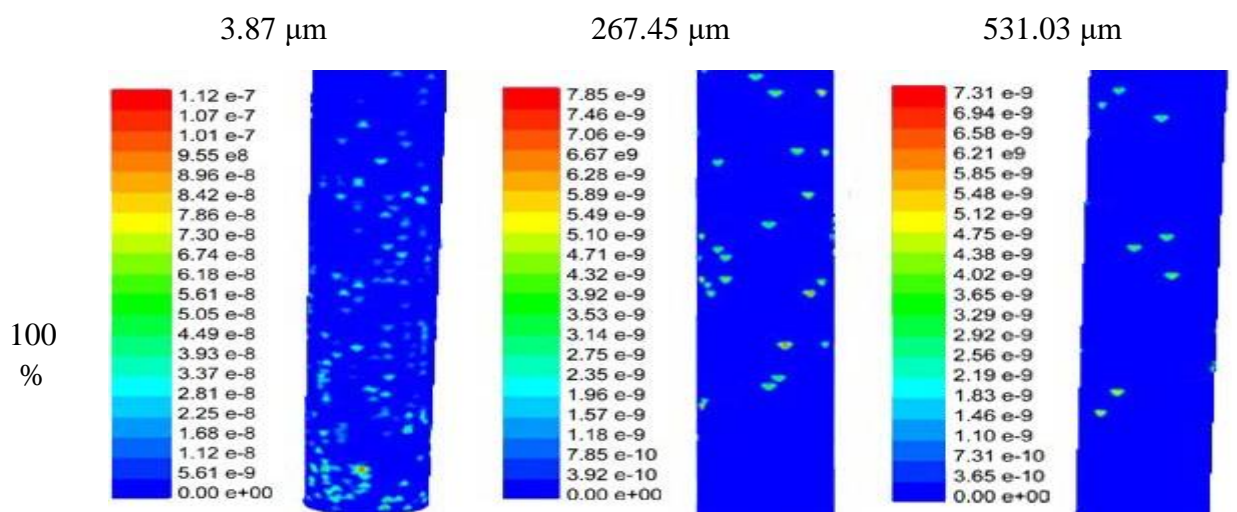


Figure.8. Effects of particle diameter on ER for 6% of particle concentration

6. Conclusion

A three-dimensional fluid–structure interaction computational model coupling with a combined continuum and discrete model has been used to predict the erosion rate the flow field distribution of gas particle. flow and the erosion rate of valve body and core are captured under different operating and structural conditions with different fluid parameters. From the descriptions above, the following conclusions can be drawn :

1- With increase of particle diameter in 25%, 50% and 75% open states of ball valve, the rate of erosion is increased. On the contrary, opposite rule governs in complete open state of ball valve. That is, the rate of erosion is decreased with increase in particle diameter.

2- In all four ball states, the erosion area is decreased with increase of particle diameters.

7. References

- [1] K. Haugen, O. Kvernfold, A. Ronold, R. Sandberg, Sand erosion of wear-resistant materials: Erosion in choke valves, *Wear*, Vol. 186, pp. 179-188, 1995.
- [2] B. McLaury, J. Wang, S. Shirazi, J. Shadley, E. Rybicki, Solid particle erosion in long radius elbows and straight pipes, in *Proceeding of, Society of Petroleum Engineers*, pp.
- [3] A. Forder, M. Thew, D. Harrison, A numerical investigation of solid particle erosion experienced within oilfield control valves, *Wear*, Vol. 216, No. 2, pp. 184-193, 1998.
- [4] G. Parslow, D. Stephenson, J. Strutt, S. Tetlow, Investigation of solid particle erosion in components of complex geometry, *Wear*, Vol. 233, pp. 737-745, 1999.
- [5] A. Kavner, T. S. Duffy, G. Shen, Phase stability and density of FeS at high pressures and temperatures: implications for the interior structure of Mars, *Earth and Planetary Science Letters*, Vol. 185, No. 1, pp. 25-33, 2001.
- [6] J. Jin, J. Fan, X. Zhang, K. Cen, Numerical simulation of the tube erosion resulted from particle impacts, *Wear*, Vol. 250, No. 1, pp. 114-119, 2001 .
- [7] J. Fan, K. Luo, X. Zhang, K. Cen, Large eddy simulation of the anti-erosion characteristics of the ribbed-bend in gas-solid flows, *Journal of engineering for gas turbines and power*, Vol. 126, No. 3, pp. 672-679, 2004.
- [8] T. Deng, M. Patel, I. Hutchings, M. Bradley, Effect of bend orientation on life and puncture point location due to solid particle erosion of a high concentration flow in pneumatic conveyors, *Wear*, Vol. 258, No. 1, pp. 426-433, 2005.
- [9] Y. I. Oka, K. Okamura, T. Yoshida, Practical estimation of erosion damage caused by solid particle impact: Part 1: Effects of impact parameters on a predictive equation, *Wear*, Vol. 259, No. 1, pp. 95-101, 2005.
- [10] X. Chen, B. S. McLaury, S. A. Shirazi, Numerical and experimental investigation of the relative erosion severity between plugged tees and elbows in dilute gas/solid two-phase flow, *Wear*, Vol. 261, No. 7, pp. 715-729, 2006.
- [11] M. Habib, H. Badr, S. Said, R. Ben-Mansour, S. Al-Anizi, Solid-particle erosion in the tube end of the tube sheet of a shell-and-tube heat exchanger, *International journal for numerical methods in fluids*, Vol. 50, No. 8, pp. 885-909, 2006.
- [12] R. Malka, S. Nešić, D. A. Gulino, Erosion–corrosion and synergistic effects in disturbed liquid-particle flow, *Wear*, Vol. 262, No. 7, pp. 791-799, 2007.
- [13] M. Suzuki, K. Inaba, M. Yamamoto, Numerical simulation of sand erosion in a square-section 90-degree bend, *Journal of Fluid Science and Technology*, Vol. 3, No. 7, pp. 868-880, 2008.
- [14] P. Tang, J. Yang, J. Zheng, G. Ou, S. He, J. Ye, I. Wong, Y. Ma, Erosion-corrosion failure of REAC pipes under multiphase flow, *Frontiers of Energy and Power Engineering in China*, Vol. 3, No. 4, pp. 389-395, 2009.

- [15] Y. M. Ferng, B. H. Lin, Predicting the wall thinning engendered by erosion–corrosion using CFD methodology, *Nuclear Engineering and Design*, Vol. 240, No. 10, pp. 2836-2841, 2010.
- [16] R. Li, A. Yamaguchi, H. Ninokata, Computational fluid dynamics study of liquid droplet impingement erosion in the inner wall of a bent pipe, *Journal of Power and Energy Systems*, Vol. 4, No. 2, pp. 327-336, 2010.
- [17] B. Yan, H. Gu, L. Yu, CFD analysis of the loss coefficient for a 90° bend in rolling motion, *Progress in Nuclear Energy*, Vol. 56, pp. 1-6, 2012.
- [18] H. Zhang, Y. Tan, D. Yang, F. X. Trias, S. Jiang, Y. Sheng, A. Oliva, Numerical investigation of the location of maximum erosive wear damage in elbow: Effect of slurry velocity, bend orientation and angle of elbow, *Powder Technology*, Vol. 217, pp. 467-476, 2012. “(in Persian)”
- [19] M. Shahbazi, S. Noori zadeh, Identification of Black Powder in Natural Gas Transmission Network, in *The third scientific conference on process engineering (oil, gas refining and petrochemicals)*, Tehran, 2014. “(in Persian)”
- [20] D. SHAFEE, K. KHORSHIDI, K. M. MORAVEJI, Numerical Analysis of Erosion/Corrosion due to Gas Flow in Pipelines and Gas Stations, 2014.
- [21] H. Zhu, Q. Pan, W. Zhang, G. Feng, X. Li, CFD simulations of flow erosion and flow-induced deformation of needle valve: Effects of operation, structure and fluid parameters, *Nuclear Engineering and Design*, Vol. 273, pp. 396-411, 2014.
- [22] M. Droubi, R. Tebowei, S. Islam, M. Hossain, E. Mitchell, Computational Fluid Dynamic Analysis of Sand Erosion in 90° Sharp Bend Geometry, 2016.